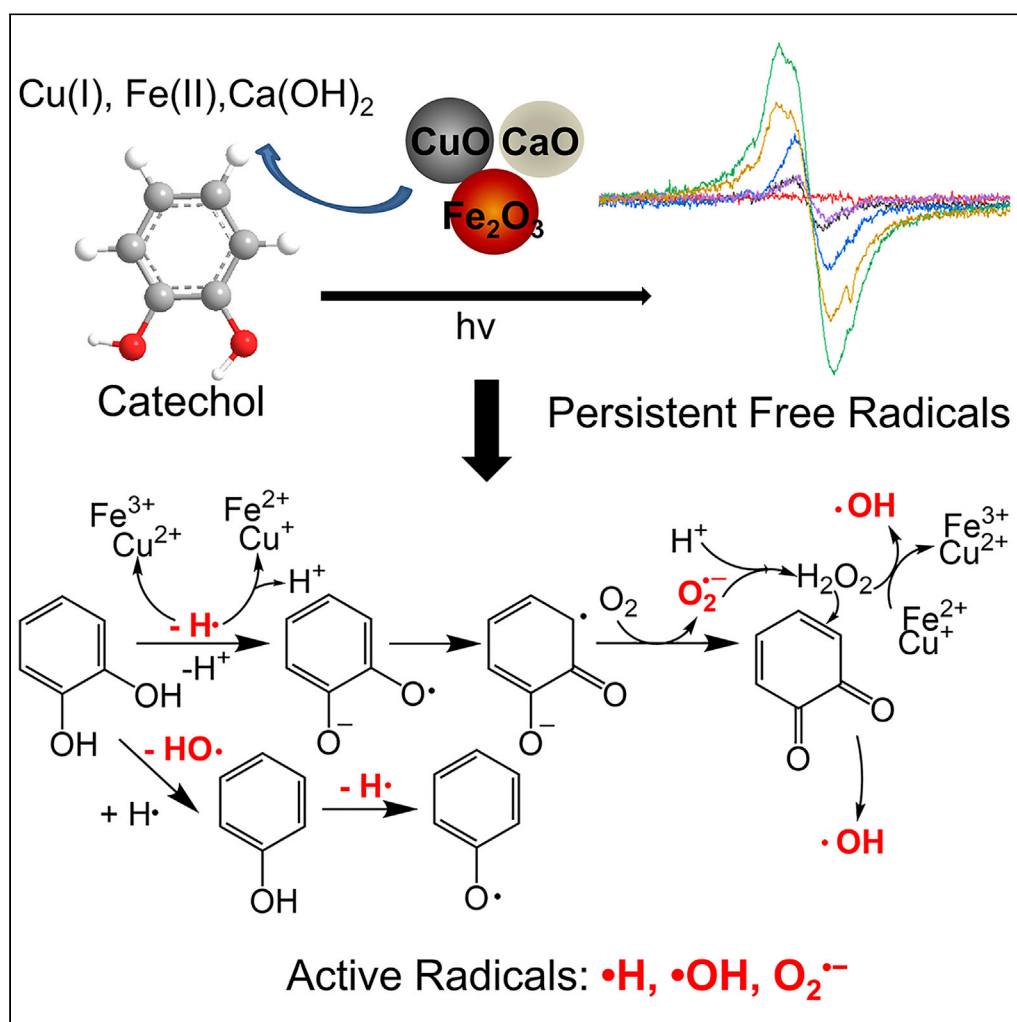


## Article

## Photoinduced formation of persistent free radicals, hydrogen radicals, and hydroxyl radicals from catechol on atmospheric particulate matter



Linjun Qin, Lili Yang, Jiahui Yang, ..., Cui Li, Minghui Zheng, Guorui Liu

griiu@rcees.ac.cn

## HIGHLIGHTS

Photochemical mechanism of persistent free radicals from catechol was clarified

Significant free radicals were formed via photochemical reactions of catechol

•H and O<sub>2</sub>•<sup>-</sup> were first discovered from the photochemical reactions of catechol

This study is important for better recognizing DNA damage of air inhalation of PM<sub>2.5</sub>

Qin et al., iScience 24, 102193  
March 19, 2021 © 2021 The Author(s).  
<https://doi.org/10.1016/j.isci.2021.102193>

## Article

## Photoinduced formation of persistent free radicals, hydrogen radicals, and hydroxyl radicals from catechol on atmospheric particulate matter

Linjun Qin,<sup>1,2</sup> Lili Yang,<sup>1,2</sup> Jiahui Yang,<sup>3</sup> Ralph Weber,<sup>4</sup> Kalina Ranguelova,<sup>4</sup> Xiaoyun Liu,<sup>1,2</sup> Bingcheng Lin,<sup>5</sup> Cui Li,<sup>1,2</sup> Minghui Zheng,<sup>1,2,5</sup> and Guorui Liu<sup>1,2,5,6,\*</sup>

## SUMMARY

Catechol is speculated to be a potential precursor of environmentally persistent free radicals (EPFRs) in the atmosphere. EPFRs absorbed on PM<sub>2.5</sub> have attracted public attention because their toxicity is similar to cigarette smoke. In this study, we found that catechol could produce EPFRs, which were oxygen-centered phenoxy and semiquinone radicals. These free radical species had half-lives of up to 382 days. CaO, CuO, and Fe<sub>2</sub>O<sub>3</sub> markedly promoted EPFR formation from catechol. The valence states of Cu and Fe changed during the photochemical reactions of catechol but no valence state changed for Ca. Alkaline nature of CaO is possibly the key for promoting the free radical formations through acid-base reactions with catechol. In addition to hydroxyl free radicals, hydrogen free radicals and superoxide anions formed from the photochemical reactions of catechol were first discovered. This is of concern because of the adverse effects of these free radicals on human health.

## INTRODUCTION

Catechol is an important organic chemical that is intentionally manufactured and used as a chemical intermediate, antibacterial agent, and industrial additive in rubber production, adhesive, galvanizing, preservatives, pesticides, and production of epinephrine (Bhuiyan et al., 2020; Esguerra, 2017; Sedo et al., 2013). Catechol can be unintentionally produced and released from full-scale industrial activities such as metallurgy, waste incineration, and chemical manufacture. Catechol is also a natural polyphenolic compound that is present in a wide range of plants such as tea, vegetables, and fruits (Sun Yugang et al., 2000). Plants and lignin decomposition are important sources of catechol in the atmosphere and other environment compartments. Moreover, catechol can be formed by daily human activities such as cooking and household heating by combustion of coal or biomass (Kibet et al., 2015; Sedo et al., 2013). Catechol emissions to the atmosphere through biomass burning were investigated and the average emission ratio of benzenediols (catechol, resorcinol) to CO was 0.37 mmol mol/CO by using the predominant vegetation at two California facilities as fuels (Veres et al., 2010). The total concentrations of phenols in the rainwater ranged from 0 to 1383 µg/L in the east of France (Schummer et al., 2009). Thus, catechol is a ubiquitous organic precursor in the environment, and it can arise from various anthropogenic activities.

Phenols are important precursors for the formation of many highly toxic organic pollutants, including the notorious carcinogenic dioxins (Evans and Dellinger, 2003, 2005; Nishinaga et al., 1977). Environmentally persistent free radicals (EPFRs) are emerging environmental pollutants that could potentially be formed from phenols (Burcat et al., 2003; Cook et al., 1956; Steelink, 1965). EPFRs can contribute to the formation of reactive oxygen species in simulated lung fluid (Tong et al., 2017). The health risks arising from EPFRs in fine atmospheric particulate matter (PM<sub>2.5</sub>) are reportedly similar to that of cigarette smoking and could explain why non-smokers develop cancers similar to those seen in smokers (Dellinger, 2008; Pryor et al., 1983). It has also been confirmed that EPFRs cause DNA damage (Gehling et al., 2014; Kelley et al., 2013; Khachatryan et al., 2011; Valavanidis et al., 2013). Thus, EPFRs are an emerging concern because of health risks associated with their inhalation along with PM<sub>2.5</sub> or dietary intake.

EPFRs have been detected in multiple environmental samples, including PM<sub>2.5</sub>, soil organic matter, and industrial fly ash samples (Gehling and Dellinger, 2013; Gehling et al., 2014; Jia et al., 2017; Kiruri et al., 2013; Yang

<sup>1</sup>State Key Laboratory of Environmental Chemistry and Ecotoxicology, Research Center for Eco-Environmental Sciences, Chinese Academy of Sciences, Beijing 100085, China

<sup>2</sup>College of Resource and Environment, University of Chinese Academy of Sciences, Beijing 100049, China

<sup>3</sup>Braker BioSpin Corp, Shanghai 200233, China

<sup>4</sup>Braker BioSpin Corp, Billerica, MA 01821, USA

<sup>5</sup>School of Environment, Hangzhou Institute for Advanced Study, UCAS, Hangzhou 310000, China

<sup>6</sup>Lead contact

\*Correspondence: grliu@rcees.ac.cn

<https://doi.org/10.1016/j.isci.2021.102193>



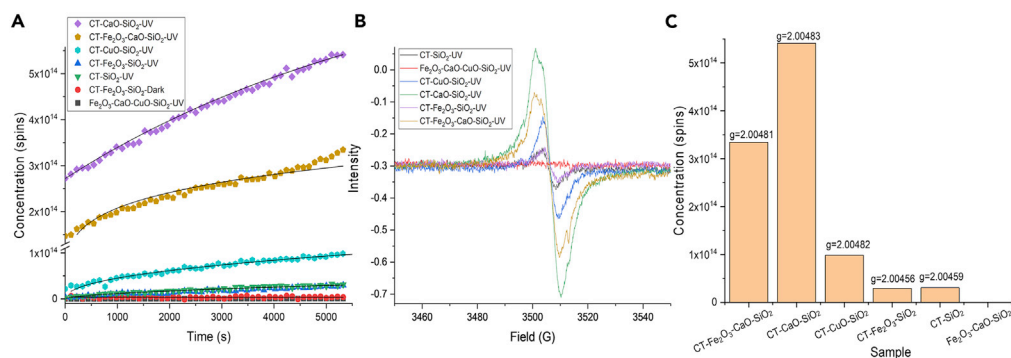


**Figure 1. The formation of EPFRs in CT/SiO<sub>2</sub> system under UV irradiation**

(A) Concentrations of EPFRs on the surface of SiO<sub>2</sub> loaded with catechol (CT) and a metal oxide (Fe<sub>2</sub>O<sub>3</sub>, CaO, or CuO) or without a metal oxide. Changes in the EPFRs with time under UV irradiation.

(B) EPR spectra for SiO<sub>2</sub> loaded with catechol (CT) and a metal oxide (Fe<sub>2</sub>O<sub>3</sub>, CaO, or CuO) or without a metal oxide after UV irradiation for 5500 s.

(C) The g values and concentrations of organic free radicals in reaction system samples after UV irradiation for 5500 s. Blank conditions: 5% Fe<sub>2</sub>O<sub>3</sub> + 5% CuO +5% CaO +85% SiO<sub>2</sub>, with UV irradiation. CT-Dark conditions: 5% catechol +5% Fe<sub>2</sub>O<sub>3</sub> + 90% SiO<sub>2</sub>, without UV irradiation.

et al., 2017a, 2017b). The two major sources of EPFRs are primary release from various anthropogenic activities and secondary formation from precursors in the environment (Yang et al., 2017a). For primary sources, EPFRs are formed and released by waste incineration, metallurgical processes, and combustion of coal and biomass (Yang et al., 2017a). Although secondary formation of EPFRs in the atmosphere is hypothesized to be likely, it is not clear if EPFRs and highly active free radicals can be formed from catechol in the atmosphere, and key factors affecting their formation are not fully understood. Organic precursors are essential for EPFR formation (Lomnicki et al., 2008; Mahmood et al., 2018; Mas-Torrent et al., 2012; Vejerano et al., 2011). Catechol is a widespread organic precursor in the environment, and the formation potential of EPFRs from catechol under natural conditions and the mechanism and influencing factors need to be clarified. Light irradiation is important for triggering the formation of EPFRs and highly active free radicals in natural environments, and especially in the atmosphere (Awwad et al., 2020; Krapf et al., 2016). It is essential to consider the effect of light irradiation on EPFR formation because it could affect secondary formation of EPFRs in the atmosphere.

In this study, catechol was selected as a typical organic precursor because it is ubiquitous in the environment. The formation potentials of EPFRs and highly active free radicals from catechol were evaluated under light irradiation and taking into consideration secondary formation of EPFRs. The results of this study could improve the understanding of the formation of EPFRs and highly active free radicals from catechol under natural conditions.

## RESULTS AND DISCUSSION

### Electron spin levels of free radicals formed from catechol by photochemical reactions

Photoinduced electron transfer is an important pathway for initiating oxidation–reduction reactions of organic precursors, including phenols. Free radicals could be involved in and formed by the photochemical reactions of organic precursors; however, the electron spin levels of free radicals formed from catechol through photochemical reactions with different sorts of metal oxide loaded need to be accurately quantified. In this study, the electron spin levels of free radicals formed from catechol under UV and visible light irradiation were evaluated taking into considering the percentages of UV (7%) and visible light (50%) in sunlight (Xu et al., 2016).

The electron spin levels of free radicals formed from catechol under UV irradiation are shown in Figure 1. Distinct signals for free radicals were detected in the experiments conducted with UV irradiation compared with without UV irradiation (Figure 1A). UV irradiation greatly increased the levels of the free radicals. These results showed that free radicals were formed from catechol through photochemical reactions under UV irradiation.

The effects of normal metal oxides, including Fe<sub>2</sub>O<sub>3</sub>, CuO, and CaO, on the generation of free radicals from catechol were studied under UV irradiation (Figure 1A). Addition of only Fe<sub>2</sub>O<sub>3</sub> to the reaction system of catechol on SiO<sub>2</sub> did not markedly promote the formation of free radicals. However, addition of CaO and

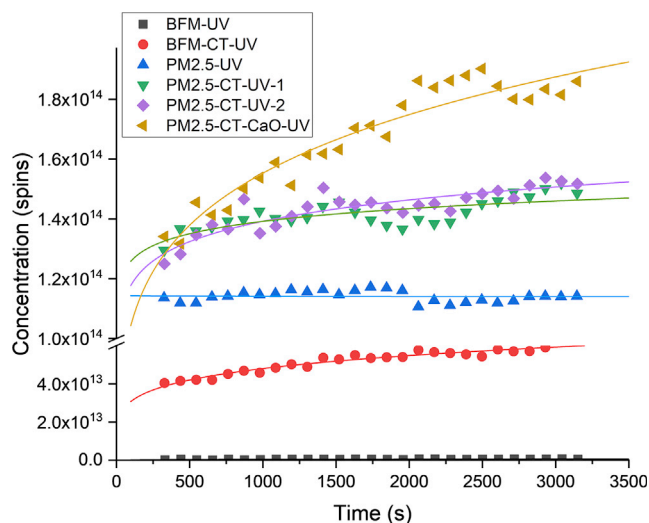


**Figure 2. The formation of EPFRs from catechol on PM<sub>2.5</sub> under UV irradiation**

Changes in the EPFR concentrations over time under continuous UV irradiation for PM<sub>2.5</sub> loaded with catechol (CT, 10%). PM<sub>2.5</sub>/CT-UV-1 and PM<sub>2.5</sub>/CT-UV-2 were conducted in parallel.

BFM: blank filter membrane.

CuO to the reaction system greatly increased the electron paramagnetic resonance spectroscopy (EPR) signal. In a previous study, the higher oxidation potential of Fe<sub>2</sub>O<sub>3</sub> resulted in greater decomposition of the adsorbate, which led to lower EPFR yields (Vejerano et al., 2011). This supported our observations in the present study. In thermochemical reaction system, CuO may act as an important surface catalyst and could mediate the EPFR formation (Lomnicki et al., 2008). When CaO was added to the reaction system, the phenol decomposition rate markedly increased, and the reaction time decreased by 2.1–2.6 times (Shin et al., 2020). CaO could absorb CO<sub>2</sub> and H<sub>2</sub>O produced during pyrolysis of biomass and reduce the activation energy required for the reaction, which would promote the pyrolysis (Wang et al., 2020). In this study, CaO also greatly enhanced the reactivity of catechol.

There are distinct differences between UV and visible light, with the energy of visible light being lower than that of UV. Therefore, we also evaluated the formation of free radicals from catechol under visible light irradiation. Under visible light irradiation, free radicals were produced from catechol on Fe<sub>2</sub>O<sub>3</sub>/SiO<sub>2</sub> (Figure S1). More free radicals were produced as the visible light irradiation period increased. Continual UV irradiation for 5000 s gave an EPFR yield in catechol/Fe<sub>2</sub>O<sub>3</sub>/SiO<sub>2</sub> that was three times higher than that from continual visible light irradiation for 5000 s. The g values of organic free radicals in catechol/Fe<sub>2</sub>O<sub>3</sub>/SiO<sub>2</sub> after UV irradiation and visible light irradiation for 5000 s are 2.00459 and 2.00453, respectively. Therefore, different optical wavelengths have different abilities to induce formation of EPFRs.

### Formation of free radicals from catechol on PM<sub>2.5</sub> as a reaction matrix under light irradiation

The solid matrix is the key factor influencing the formation of free radicals and their stability. Under atmospheric conditions, PM<sub>2.5</sub> is a very important matrix for EPFR formation. To improve our understanding of the formation potentials of free radicals in the atmosphere with PM<sub>2.5</sub> as the reaction matrix, EPR experiments were conducted with real PM<sub>2.5</sub> samples spiked with catechol. The electron spin levels of free radicals formed on the PM<sub>2.5</sub> matrix are shown in Figure 2 and the morphologies and elemental compositions of PM<sub>2.5</sub> are shown in Figure S2. Under UV irradiation, free radicals were clearly formed from catechol on the PM<sub>2.5</sub> matrix. The amount of EPFRs formed from catechol on PM<sub>2.5</sub> was markedly higher than that formed from catechol without PM<sub>2.5</sub> as a reaction matrix. This suggests that EPFRs in the atmosphere are mainly formed in the solid PM phase. Furthermore, the electron spin levels for the PM<sub>2.5</sub> spiked with catechol were higher than those for PM<sub>2.5</sub> without catechol. These results indicate that catechol in the atmosphere could contribute greatly to the formation of free radicals on PM<sub>2.5</sub>.

It is widely recognized that CaO is a possible inhibitor of organic pollutant formation (Liu et al., 2005). However, it is unclear whether CaO can inhibit free radical formation or not. Thus, we also evaluated the electron

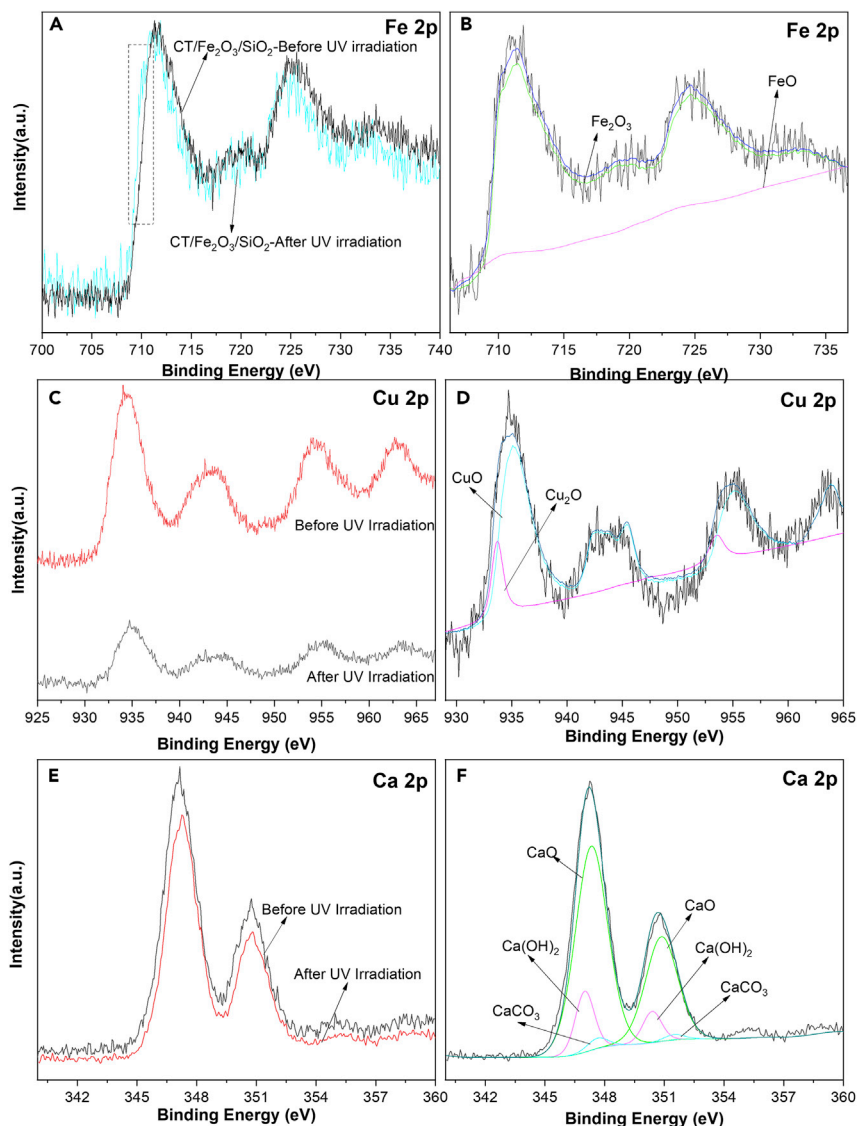


**Figure 3. The XPS results**

XPS of (A) catechol (CT)/Fe<sub>2</sub>O<sub>3</sub>/SiO<sub>2</sub> Fe 2p, (B) deconvolution of the Fe 2p spectrum of CT/Fe<sub>2</sub>O<sub>3</sub>/SiO<sub>2</sub> after UV irradiation. (C) CT/CuO/SiO<sub>2</sub> Cu 2p spectrum. (D) deconvolution of the Cu 2p spectrum of CT/CuO/SiO<sub>2</sub> after UV irradiation. (E) CT/CaO/SiO<sub>2</sub> Ca 2p spectrum, and (F) deconvolution of the Ca 2p spectrum of CT/CaO/SiO<sub>2</sub> after UV irradiation.

spin levels of free radicals after addition of CaO to the PM<sub>2.5</sub>/catechol/UV irradiation system. The electron spin levels of the free radicals unexpectedly increased after addition of CaO to the reaction system (Figure 2). Therefore, instead of inhibiting free radical formation, CaO promotes the generation of free radicals in the catechol/PM<sub>2.5</sub>/UV irradiation system. This is important knowledge for those considering the potential of applying CaO to inhibition of free radical formation.

### XPS characterization and the influencing mechanisms of metal oxides on free radical formations from catechol

To improve our understanding of the role of metal oxides in free radical formation by photochemical reactions, X-ray photoelectron spectroscopy (XPS) was used to characterize changes in the metal oxides before and after UV irradiation. For catechol/Fe<sub>2</sub>O<sub>3</sub>/SiO<sub>2</sub>, XPS of the Fe 2P region showed a change in low binding energy peak (710 eV–712.5 eV) after UV irradiation (Figure 3A). Furthermore, comparison of the characteristic Fe 2p peaks of Fe<sub>2</sub>O<sub>3</sub> and FeO to those in the catechol/Fe<sub>2</sub>O<sub>3</sub>/SiO<sub>2</sub> sample after UV

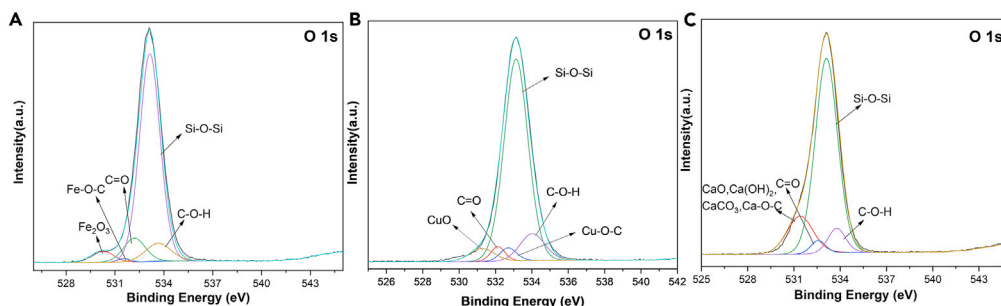


**Figure 4. The XPS spectra and deconvolution of the O 1s spectra**

The O 1s spectra of (A) catechol (CT)/Fe<sub>2</sub>O<sub>3</sub>/SiO<sub>2</sub>, (B) CT/CuO/SiO<sub>2</sub>, and (C) CT/CaO/SiO<sub>2</sub> after UV irradiation

irradiation (Figure 3B) showed that Fe<sup>3+</sup> accounted for 91.57% and Fe<sup>2+</sup> for 8.43% of the total Fe. The XPS spectrum of Cu 2p for catechol/CuO/SiO<sub>2</sub> is shown in Figure 3C. After deconvolution of the Cu 2p spectrum of catechol/CuO/SiO<sub>2</sub> after UV irradiation (Figure 3D), the characteristic Cu 2p peaks of CuO and Cu<sub>2</sub>O showed that Cu<sup>2+</sup> accounted for 80.3% and Cu<sup>+</sup> for 19.7% of the total Cu. The changes in the chemical states characterized by XPS indicated that Fe(III) was reduced to Fe(II) and Cu(II) to Cu(I). This suggested that electron transfer from catechol to Fe<sub>2</sub>O<sub>3</sub> and CuO occurred during the photochemical reactions, and that Fe<sub>2</sub>O<sub>3</sub> and CuO participated in the EPFR formation reactions. In the Ca 2p<sub>3/2</sub> spectrum of CaO/catechol/SiO<sub>2</sub> before and after the photochemical reactions, peaks were observed for Ca<sup>2+</sup>O at 347.41 eV and Ca<sup>2+</sup>(OH)<sub>2</sub> at 346.91 eV (Figures 3E, 3F, and S3). (Sugama et al., 1989; Vandoveren and Verhoeven, 1980) The proportion of Ca(OH)<sub>2</sub> increased from 7% before the photochemical reactions to 15% after the photochemical reactions, which suggested that the EPFRs formed via elimination of H<sub>2</sub>O in a photochemical reaction of catechol with a metal oxide (Lomnicki et al., 2008). It has been reported that CaO can reduce the activation energy required for a reaction in the reaction system and restored system activity, which might also contribute to its ability to promote formation of EPFRs (Wang et al., 2020; Wiechen et al., 2012).

The XPS O 1s spectrum of the catechol/Fe<sub>2</sub>O<sub>3</sub>/SiO<sub>2</sub>, catechol/CuO/SiO<sub>2</sub>, and catechol/CaO/SiO<sub>2</sub> reaction systems are shown in Figure 4. The XPS O 1s spectrum of the catechol/Fe<sub>2</sub>O<sub>3</sub>/SiO<sub>2</sub> system after UV irradiation could be deconvoluted into five peaks at 533.14 eV (Si-O-Si of SiO<sub>2</sub>), 532.20 eV (C=O of benzoquinone), 531.54 eV (Fe-O-C), 530.23 eV (Fe<sub>2</sub>O<sub>3</sub>), and 533.68 eV (C-O-H of phenolic hydroxyl) for (Figure 4A) according to the literature (Barr, 1983; Kishi and Ikeda, 1973; Lhoest et al., 1995; Trinh et al., 2018; Xie et al., 2020). The XPS O 1s spectrum of the catechol/CuO/SiO<sub>2</sub> system could be deconvoluted into five peaks at 533.13 eV (Si-O-Si of SiO<sub>2</sub>), 532.13 eV (C=O of benzoquinone), 532.70 eV (Cu-O-C), 531.27 eV (CuO), and 534.03 eV (C-O-H of phenolic hydroxyl) (Figure 4B). (Barr, 1983; Cebula et al., 2013; Lhoest et al., 1995; Nefedov et al., 1982; Trinh et al., 2018) The peaks at 531.54 for Fe-O-C and 532.84 eV for Cu-O-C correspond to hydroxyl species from catechol on the Fe<sub>2</sub>O<sub>3</sub> and CuO surfaces. Therefore, complete electron transfer occurred and Fe-O-C and Cu-O-C bonds formed during the photochemical reactions for EPFR formation. The XPS O 1s spectrum of catechol/CaO/SiO<sub>2</sub> could be deconvoluted into five peaks at 533.11 eV (Si-O-Si of SiO<sub>2</sub>), 532.50 eV (C=O of benzoquinone), 533.77 eV (C-O-H of phenolic hydroxyl), and 531.4 eV for CaO, Ca(OH)<sub>2</sub>, CaCO<sub>3</sub>, and Ca-O-C because of their similar binding energies (Figure 4C). (Barr, 1983; Lhoest et al., 1995; Sugama et al., 1989; Trinh et al., 2018)

### Identification of highly active free radicals formed from photochemical reactions of catechol

Besides EPFRs, highly active free radicals were also investigated in this study. Free radical trapping was used to identify the active free radicals produced from catechol. DMPO in aqueous solution was used as a trapping agent to detect any active free radicals. Hydroxyl free radicals can reportedly form from EPFRs in PM<sub>2.5</sub> (Gehling et al., 2014). In this study, besides hydroxyl free radicals, the formation and occurrence of hydrogen free radicals from the photochemical reactions of catechol and PM<sub>2.5</sub> were discovered for the first time. The EPR spectra are shown in Figure 5 and the fitting results are shown in Figures 6 and S4.

DMPO–OH adducts with a splitting of  $\alpha_N = \alpha_H = 14.7$  G (literature data  $\alpha_N = \alpha_H = 14.9$  G) (Rosen and Rauckman, 1981) were detected in the catechol/SiO<sub>2</sub> sample after UV irradiation (Figure 5). DMPO–H adducts

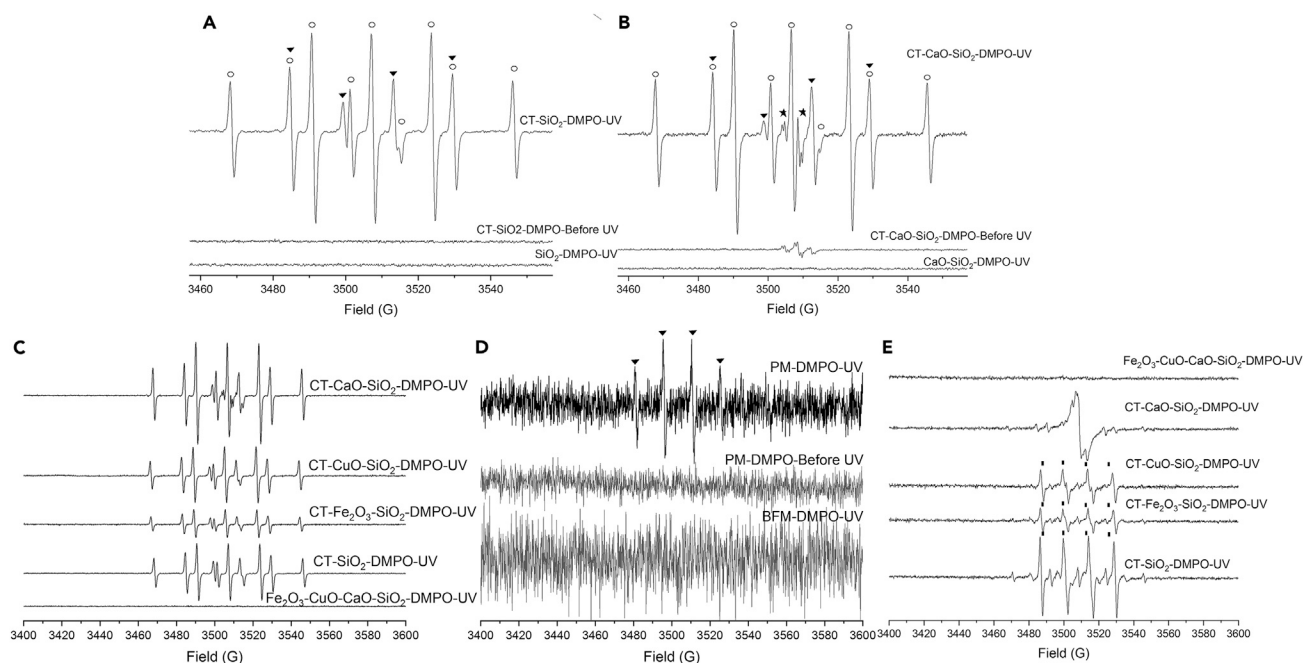


**Figure 5. EPR spectra of spin-trapped radicals detected in the experiments with the following conditions**

(A) 2  $\mu$ L, 3 M DMPO + 30  $\mu$ L, PBS + 2.5 mg of catechol (CT)/SiO<sub>2</sub> with UV irradiation for 20 s, control: 2  $\mu$ L, 3 M DMPO/water + 30  $\mu$ L, PBS + 2.5 mg of SiO<sub>2</sub> with UV irradiation;

(B) 2  $\mu$ L, 3 M DMPO + 30  $\mu$ L, PBS + 2.5 mg of CT/CaO/SiO<sub>2</sub> with UV irradiation, control: 2  $\mu$ L, 3 M DMPO/water + 30  $\mu$ L, PBS + 2.5 mg of CaO/SiO<sub>2</sub> with UV irradiation;

(C) 2  $\mu$ L, 3 M DMPO/water + 30  $\mu$ L, PBS + 2.5 mg of CT/SiO<sub>2</sub>/metal oxide (Fe<sub>2</sub>O<sub>3</sub>, CuO, CaO) with UV irradiation;

(D) 2  $\mu$ L, 3 M DMPO/water + 30  $\mu$ L, PBS + 1 mg of PM<sub>2.5</sub> with UV irradiation, control: 2  $\mu$ L, 3 M DMPO + 30  $\mu$ L, PBS + 1 mg of BFM with UV irradiation;

(E) 2  $\mu$ L, 3 M DMPO + 2.5 mg of CT/SiO<sub>2</sub>/metal oxide (Fe<sub>2</sub>O<sub>3</sub>, CuO, CaO) with UV irradiation, control: 2  $\mu$ L, 3 M DMPO + 2.5 mg of Fe<sub>2</sub>O<sub>3</sub>/CuO/CaO/SiO<sub>2</sub> with UV irradiation.

Symbols: ○, DMPO-H; ▼, DMPO-OH; ■, DMPO-OOH; ★, EPFR.

with splitting of  $\alpha_N = 16.5$  G and  $\alpha_H = 22.5$  G (literature data  $\alpha_N = 16.6$  G and  $\alpha_H = 22.5$  G) (Makino et al., 1982) were detected in the catechol/SiO<sub>2</sub> EPFRs system after UV irradiation. The direct scission of chemical bonds by UV irradiation was responsible for EPFR photochemical formation. Elimination of  $\cdot$ H means more oxygen-containing functional groups will be produced in the catechol-SiO<sub>2</sub> system, which might contribute to the formation of phenoxy and semiquinone radicals. Density functional theory calculation was used to verify EPFRs formed by hydrogen (H) abstraction of phenolic precursor in silico study (Dellinger et al., 2007; Yang et al., 2017b). This also supported our observations in the present study.

After the addition of CaO to the catechol-SiO<sub>2</sub> system (Figure 5C), more  $\cdot$ H and  $\cdot$ OH were produced and this suggested that CaO may promote the production of  $\cdot$ H and  $\cdot$ OH in this system under light irradiation. In addition, the yield of EPFRs from the catechol/CaO/SiO<sub>2</sub> system was much higher than that from the catechol/SiO<sub>2</sub> system. These results indicate that CaO possible promotes the formation of EPFRs by facilitating the eliminating of  $\cdot$ H and  $\cdot$ OH from catechol. The XPS results for Ca(OH)<sub>2</sub> after UV irradiation also provided further evidence for this mechanism. Interestingly, during the detection of  $\cdot$ H and  $\cdot$ OH by EPR, a hyperfine signal was observed with a splitting of  $\alpha_{H1} = 0.77$  G and  $\alpha_{H2} = -3.69$  G (literature data:  $\alpha_{H1} = 0.96$  G and  $\alpha_{H2} = -3.50$  G) (Gerson and Huber W, 2003), which indicated the existence of *o*-benzosemiquinone in the catechol/CaO/SiO<sub>2</sub> system in accordance with the g2 type radicals in a Xenon fitting experiment. Oxygen free radicals (O<sub>2</sub><sup>•-</sup>) with splitting of  $\alpha_N = 14.3$  G,  $\alpha_H^\beta = 12.5$  G and  $\alpha_H^{\beta1} = 0.8$  G (literature data:  $\alpha_N = 14.3$  G,  $\alpha_H^\beta = 11.7$  G and  $\alpha_H^{\beta1} = 1.2$  G) (Makino et al., 1982) was also detected in the solid phase of catechol/SiO<sub>2</sub> both with and without Fe<sub>2</sub>O<sub>3</sub> and CuO (Figures 5E and S4). The O<sub>2</sub><sup>•-</sup> in the catechol/CaO/SiO<sub>2</sub> system was markedly lower than in the other systems, which indicated that the EPFRs formed in the catechol/CaO/SiO<sub>2</sub> system were not easy to oxidize with O<sub>2</sub>. Generally,  $\cdot$ H and reactive oxygen species, including O<sub>2</sub><sup>•-</sup> and  $\cdot$ OH, can be formed in a catechol/SiO<sub>2</sub> EPFR system under UV irradiation. The free radicals  $\cdot$ H and  $\cdot$ OH were mostly formed when the system was spiked with 30  $\mu$ L of a DMPO aqueous solution,

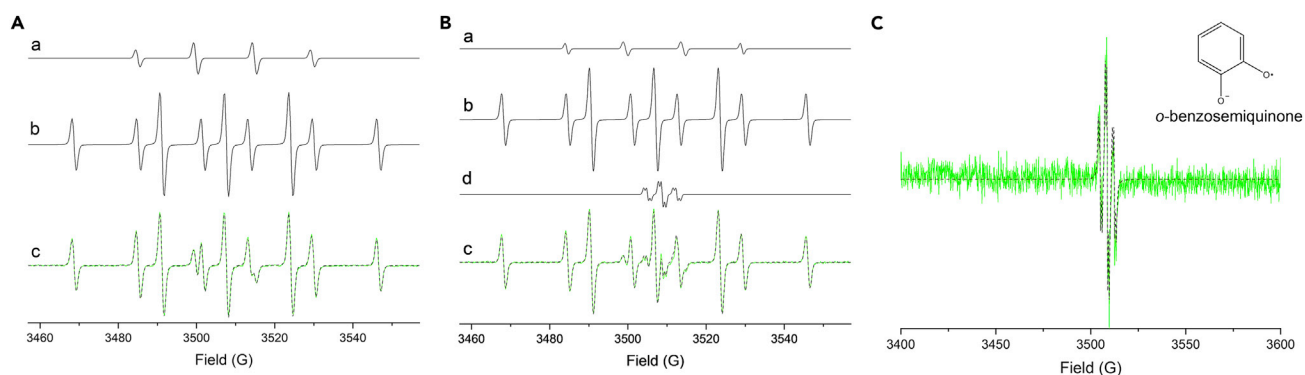


**Figure 6. Fitting of the EPR spectra of spin-trapped radicals**

(A–C)(A) spin-trapped radicals detected in catechol (CT)/SiO<sub>2</sub> under UV irradiation. (B) spin-trapped radicals detected in CT/CaO/SiO<sub>2</sub> under UV irradiation. (C) a suspension of CT/CaO/SiO<sub>2</sub>. (a) Simulated DMPO-OH adducts. (b) Simulated DMPO-H adducts. (c) Fitting of experimental (green line) and simulated (black line) EPR spectra. (d) EPFR signal.

which was considered a liquid-phase system. By contrast, O<sub>2</sub><sup>•−</sup> was mostly formed when the system was spiked with only 2 μL of DMPO solution and was considered a solid-phase system. A previous study reported the abilities of the EPFRs in PM<sub>2.5</sub> to generate •OH (Gehling et al., 2014). In this study, •OH was also detected in PM<sub>2.5</sub> after UV irradiation (Figures 5D and S5). The •OH formed in PM<sub>2.5</sub> after UV irradiation may be generated through photochemical reactions of organic pollutants like phenols. This is the first report of •H and O<sub>2</sub><sup>•−</sup> in such a reaction system and this knowledge is important for understanding their potential mechanisms and health effects.

### Structural identification and mechanism of EPFRs and their stabilities

The photochemical reaction of catechol on Fe<sub>2</sub>O<sub>3</sub>/SiO<sub>2</sub> could generate persistent radicals under visible light or UV irradiation (Figure 7). In the mixture of catechol and Fe<sub>2</sub>O<sub>3</sub>/SiO<sub>2</sub> under visible light irradiation, the *g* value changed from 2.0045 before irradiation to 2.00485 after irradiation. On the fourth day after irradiation, the *g* value remained at 2.00487 and the peak pattern did not change markedly, which indicated that oxygen-centered radicals were formed during visible light irradiation.

The spectra were complex, indicating the presence of more than one type of radical. Three different radicals were suggested when Xenon software was used to mathematically deconvolute the EPR spectra (Figure 7 and Table S1), which were denoted as *g*<sub>1</sub>, *g*<sub>2</sub>, and *g*<sub>3</sub> with *g*-values of approximately 2.0010–2.0020, 2.0040–2.0050, and >2.0050, respectively. The EPR spectral deconvolution suggested there were metal F-centers (*g*<sub>1</sub>) in the reaction systems spiked with Fe<sub>2</sub>O<sub>3</sub>, CuO, and CaO after UV irradiation and the F-center formed in CaO was similar to that for alkali halides (Henderson et al., 1969) and different from those for heavy metal oxides (CuO and Fe<sub>2</sub>O<sub>3</sub>) (Figure S6). Two types of free radicals formed on the surfaces of silica (*g*<sub>2</sub> and *g*<sub>3</sub>), which were mainly oxygen-centered phenoxy and semiquinone radicals.

The possible mechanism of the formation of EPFR under UV irradiation was shown in Figure 8. Through taking off •H and •OH from catechol, the resonance stabilized radicals including *o*-semiquinone, phenoxy and carbon-centered radicals were formed. The concentration of •H was higher than •OH, indicating that more *o*-semiquinone were formed comparing to phenoxy and carbon-centered radicals which were consistent with the deconvolution results of EPFR spectrum (Pathway 1). Apart from the direct and sequential electron transfer from the O 2p orbitals of the phenolic oxygen in catechol to Fe(III) and Cu(II) (Pathway 2)(Lomnicki et al., 2008; Vejerano et al., 2011), •H reacted with electron acceptor – Fe(III) and Cu(II) and the electron transfer from •H to Fe(III) and Cu(II) which was indirect electron transfer from phenolic oxygen in catechol to Fe(III) and Cu(II) through •H (Pathway 1). The lower concentration of •H in Fe and Cu containing sample also supported our hypothesis. Moreover, O<sub>2</sub> reacted with *o*-semiquinone type EPFRs on the surface of solid and electron transferred from EPFRs to O<sub>2</sub> generated superoxide radical (Khachatryan et al., 2011). However, the possible mechanism for CaO to promote the formation of EPFR was differed from CuO and Fe<sub>2</sub>O<sub>3</sub> and no electron transfer occurred from CT to Ca<sup>2+</sup>. CaO belonged to strong alkaline oxide,

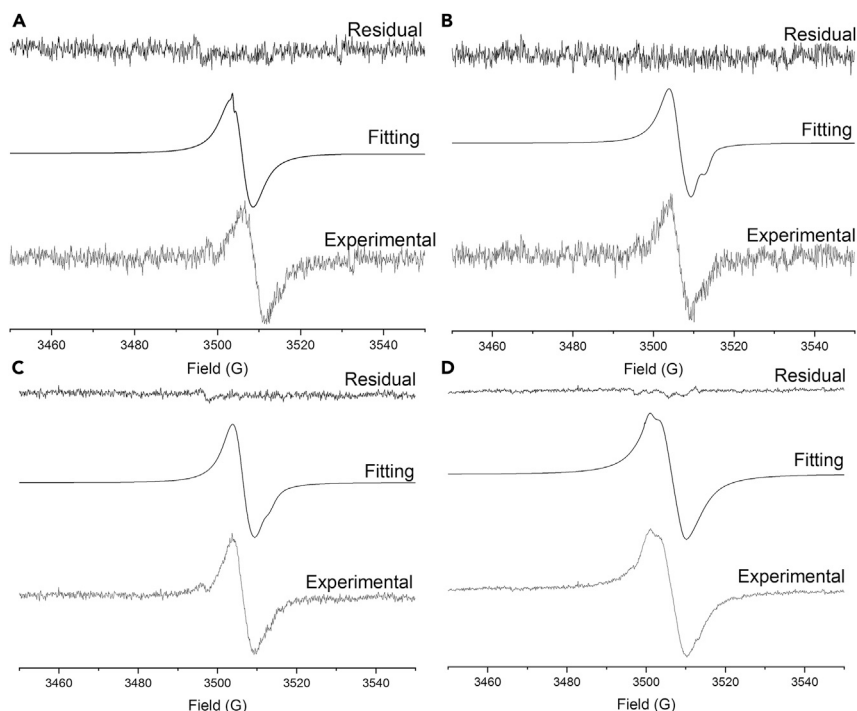


**Figure 7. Fitting of the EPR spectra**  
(A–D)(A) catechol (CT)/SiO<sub>2</sub>, (B) CT/Fe<sub>2</sub>O<sub>3</sub>/SiO<sub>2</sub>, (C) CT/CuO/SiO<sub>2</sub>, and (D) CT/CaO/SiO<sub>2</sub> during photochemical reactions after spectral deconvolution.

and catechol was weak acid in which proton hydrogen on phenolic hydroxyl was easily removed. Although CaO reacted with proton hydrogen, a lot of energy could be released to significantly promote the reaction process followed by more  $\cdot\text{H}$  elimination, EPFR formation and H<sub>2</sub>O production.

Half-life is a key parameter for evaluating the stability of EPFRs. In this study, the  $1/e$  half-lives of the EPFRs in the samples were calculated using dynamic changes in their spin levels. The half-lives of EPFRs formed on the surfaces of SiO<sub>2</sub> and PM<sub>2.5</sub> spiked with catechol or a metal oxide ranged from days to months (Figure S7), which indicated that these radicals were persistent. The EPFRs in the PM<sub>2.5</sub>, catechol/PM<sub>2.5</sub>, and catechol/BFM systems displayed fast decay with  $1/e$  lifetimes of 9.98 hr, 3.22hr, and 12.17 hr, respectively. This was followed by slower decay with  $1/e$  lifetimes of 52.17 days, 115.74 days, and 25.85 days for the PM<sub>2.5</sub>, catechol/PM<sub>2.5</sub>, and catechol/BFM systems, respectively. Compared with catechol/PM<sub>2.5</sub> and catechol/BFM, catechol/PM<sub>2.5</sub> showed slower decay of the EPFRs, which suggested that absorption of EPFRs onto the PM<sub>2.5</sub> surface increased their stability. In the catechol/CaO/PM<sub>2.5</sub> system, the concentration of EPFR first decreased ( $1/e = 8.37$  hr) and then increased slowly without further decay. This might result from continuous formation of the EPFRs from reactions of catechol, CaO, and other complex compounds in PM<sub>2.5</sub>.

Decay processes for EPFRs generated in catechol/SiO<sub>2</sub> with or without metal oxides are shown in Figure S7 e–f. The decay characteristics of the catechol/CuO/SiO<sub>2</sub>, catechol/CaO/SiO<sub>2</sub>, and catechol/SiO<sub>2</sub> systems were almost the same with a fast decay followed by a slower decay. A fast decay followed by no decay was observed for the catechol/Fe<sub>2</sub>O<sub>3</sub>/SiO<sub>2</sub> system, which supported our previous research where we found that Fe<sub>2</sub>O<sub>3</sub> stabilized EPFRs formed in this system (Vejerano et al., 2011). The faster decay might be caused by decomposition of a phenoxy-type radical and the slow decay by decomposition of a semiquinone-type radical (Gehling and Dellinger, 2013).

## CONCLUSIONS

Catechol is a common potential precursor of EPFRs in the atmosphere and anthropogenic emissions. EPFRs are recognized internationally as an important component of PM<sub>2.5</sub> when evaluating its health risks. We found that catechol could produce large amounts of EPFRs under light irradiation. Metal oxides,

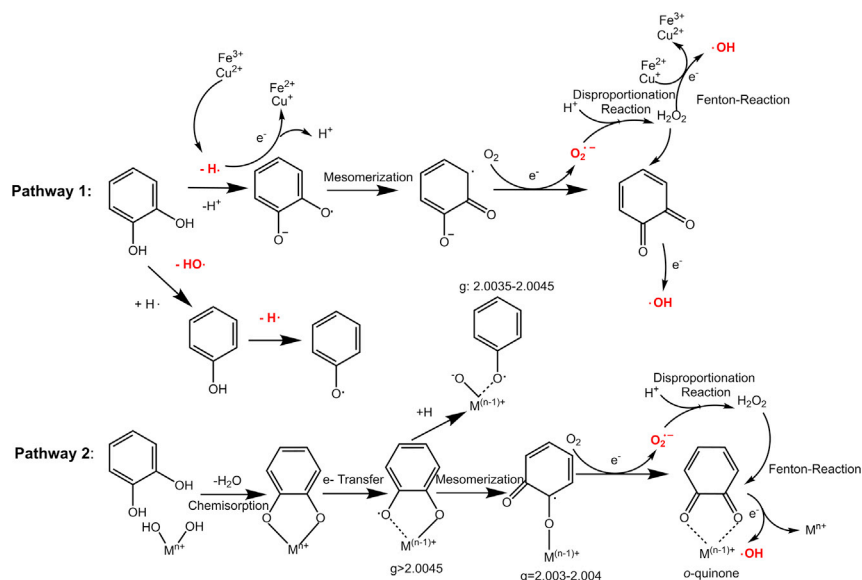


**Figure 8. Proposed mechanism for EPFR formation**

The proposed mechanism for EPFR formation accompanied by highly active free radicals participated in CT/SiO<sub>2</sub> system after UV irradiation.

including Fe<sub>2</sub>O<sub>3</sub>, CuO, and CaO, markedly promoted the formation of EPFRs from catechol, with their effects on free radical formation in the order CaO > CuO > Fe<sub>2</sub>O<sub>3</sub>. The EPFRs produced from catechol underwent relatively fast decay (1/e = 3.2–32.3 hr) followed by slower decay (25.9–382 days), which indicates that they are stable and could have potential adverse effects on human health after inhalation or dietary intake. The photochemical formation mechanism of EPFRs clarified in this study could aid understanding of their secondary formation in the atmosphere. The formation and occurrence of hydrogen free radicals from the photochemical reactions of catechol and real PM<sub>2.5</sub> were discovered for the first time. This is concerning because of their adverse effects on human health.

### Limitations of the study

Photochemical reactions of organic precursors are extremely complex in atmospheric environment. This study clarified the formation of EPFRs from catechol through photochemical reactions as well as their influencing factors. However, there are multiple precursors in the airborne particle matters. Moreover, the nature of the complexity of airborne particle matters makes it a long way to fully understand the numerous mechanisms of EPFRs from multiple potential precursors. The various factors influencing EPFR formations in atmospheric environment cannot be fully recognized in this study. Therefore, much more studies should be conducted to better understand the formation and control of EPFRs in atmospheric environment in the future.

### Resource availability

#### Lead contact

Further information and requests for resources and reagents should be directed to and will be fulfilled by the lead contact, Guorui Liu ([grliu@rcees.ac.cn](mailto:grliu@rcees.ac.cn)).

#### Materials availability

This study did not generate new unique reagents.

#### Data and code availability

This study did not generate/analyze data sets/code.

## METHODS

All methods can be found in the accompanying [Transparent Methods supplemental file](#).

## SUPPLEMENTAL INFORMATION

Supplemental information can be found online at <https://doi.org/10.1016/j.isci.2021.102193>.

## ACKNOWLEDGMENTS

This work was supported by the National Natural Science Foundation of China (grant numbers (21936007, 21906165 and 91843301), the second Tibetan Plateau Scientific Expedition and Research Program (STEP) (grant number 2019 QZKK0605), CAS Interdisciplinary Innovation Team (grant number JCTD-2019-03), and the Youth Innovation Promotion Association of the Chinese Academy of Sciences (grant number 2016038).

## AUTHOR CONTRIBUTIONS

G. L. designed the research; L. Q. conducted the experiments; L. Y., L. Q., G. L., J. Y., R. W., K. R., X. L., and C. L. analyzed the data; L. Q. and G. L. wrote the paper; L. Y, G. L., J. Y., R. W., K. R., B. L., and M. Z. revised the paper.

## DECLARATION OF INTERESTS

The authors declare no competing interests.

Received: December 14, 2020

Revised: January 14, 2021

Accepted: February 10, 2021

Published: March 19, 2021

## REFERENCES

- Awwad, N., Bui, A.T., Danilov, E.O., and Castellano, F.N. (2020). Visible-light-initiated free-radical polymerization by homomolecular triplet-triplet annihilation. *Chem* 6, 3071–3085.
- Barr, T.L. (1983). An XPS study of Si as it occurs in adsorbents, catalysts, and thin-films. *Appl. Surf. Sci.* 15, 1–35.
- Bhuiyan, M.S.A., Roland, J.D., Liu, B., Reaume, M., Zhang, Z.T., Kelley, J.D., and Lee, B.P. (2020). In situ deactivation of catechol-containing adhesive using electrochemistry. *J. Am. Chem. Soc.* 142, 4631–4638.
- Burcat, A., Khachatryan, L., and Dellinger, B.L. (2003). Thermodynamics of chlorinated phenols, polychlorinated dibenzo-p-dioxins, polychlorinated dibenzofurans, derived radicals, and intermediate species. *J. Phys. Chem. Ref. Data* 32, 443–517.
- Cebula, I., Lu, H., Zharnikov, M., and Buck, M. (2013). Monolayers of trimesic and isophthalic acid on Cu and Ag: the influence of coordination strength on adsorption geometry. *Chem. Sci.* 4, 4455–4464.
- Cook, C.D., Kuhn, D.A., and Fianu, P. (1956). Oxidation of hindered phenols. 4. Stable phenoxy radicals. *J. Am. Chem. Soc.* 78, 2002–2005.
- Dellinger, B. (2008). Newly Detected Air Pollutant Mimics Damaging Effects of Cigarette Smoke (American Chemical Society 236th National Meeting).
- Dellinger, B., Lomnicki, S., Khachatryan, L., Maskos, Z., Hall, R.W., Adoukpe, J., McFerrin, C., and Truong, H. (2007). Formation and stabilization of persistent free radicals. *Proc. Combust. Inst.* 31, 521–528.
- Esguerra, K.V.N. (2017). Phenol functionalization inspired by melanogenesis. *Chem* 2, 451–453.
- Evans, C.S., and Dellinger, B. (2003). Mechanisms of dioxin formation from the high-temperature pyrolysis of 2-chlorophenol. *Environ. Sci. Technol.* 37, 1325–1330.
- Evans, C.S., and Dellinger, B. (2005). Formation of bromochlorodibenzo-p-dioxins and furans from the high-temperature pyrolysis of a 2-chlorophenol/2-bromophenol mixture. *Environ. Sci. Technol.* 39, 7940–7948.
- Gehling, W., and Dellinger, B. (2013). Environmentally persistent free radicals and their lifetimes in PM<sub>2.5</sub>. *Environ. Sci. Technol.* 47, 8172–8178.
- Gehling, W., Khachatryan, L., and Dellinger, B. (2014). Hydroxyl radical generation from environmentally persistent free radicals (EPFRs) in PM<sub>2.5</sub>. *Environ. Sci. Technol.* 48, 4266–4272.
- Gerson, F., and Huber, W. (2003). *Electron Spin Resonance Spectroscopy of Organic Radicals* (Wiley-VCH Verlag GmbH & Co. KGaA).
- Henderson, B., Stokowski, S.E., and Ensign, T.C. (1969). Luminescence for F centers in calcium oxide. *Phys. Rev.* 183, 826+.
- Jia, H., Zhao, S., Nulaji, G., Tao, K., Wang, F., Sharma, V.K., and Wang, C. (2017). Environmentally persistent free radicals in soils of past coking sites: distribution and stabilization. *Environ. Sci. Technol.* 51, 6000–6008.
- Kelley, M.A., Hebert, V.Y., Thibeaux, T.M., Orchard, M.A., Hasan, F., Cormier, S.A., Thevenot, P.T., Lomnicki, S.M., Varner, K.J., Dellinger, B., et al. (2013). Model combustion-generated particulate matter containing persistent free radicals redox cycle to produce reactive oxygen species. *Chem. Res. Toxicol.* 26, 1862–1871.
- Khachatryan, L., Vejerano, E., Lomnicki, S., and Dellinger, B. (2011). Environmentally persistent free radicals (EPFRs). 1. Generation of reactive oxygen species in aqueous solutions. *Environ. Sci. Technol.* 45, 8559–8566.
- Kibet, J.K., Khachatryan, L., and Dellinger, B. (2015). Phenols from pyrolysis and co-pyrolysis of tobacco biomass components. *Chemosphere* 138, 259–265.
- Kiruri, L.W., Dellinger, B., and Lomnicki, S. (2013). Tar balls from Deep Water Horizon oil spill: environmentally persistent free radicals (EPFR) formation during crude weathering. *Environ. Sci. Technol.* 47, 4220–4226.
- Kishi, K., and Ikeda, S. (1973). X-ray photoelectron spectroscopic study for reaction of evaporated iron with O<sub>2</sub> and H<sub>2</sub>O. *Bull. Chem. Soc. Jpn.* 46, 341–345.
- Krapf, M., El Haddad, I., Bruns, Emily A., Molteni, U., Daellenbach, Kaspar R., Prévôt, André S.H., Baltensperger, U., and Dommen, J. (2016). Labile peroxides in secondary organic aerosol. *Chem* 1, 603–616.
- Lhoest, J.B., Bertrand, P., Weng, L.T., and Dewez, J.L. (1995). Combined time-of-flight secondary-ion mass-spectrometry and X-ray photoelectron-spectroscopy study of the surface segregation of poly(methyl methacrylate) (PMMA) in bisphenol-

- A polycarbonate PMMA blends. *Macromolecules* 28, 4631–4637.
- Liu, W., Zheng, M., Zhang, B., Qian, Y., Ma, X., and Liu, W. (2005). Inhibition of PCDD/Fs formation from dioxin precursors by calcium oxide. *Chemosphere* 60, 785–790.
- Lomnicki, S., Truong, H., Vejerano, E., and Dellinger, B. (2008). Copper oxide-based model of persistent free radical formation on combustion-derived particulate matter. *Environ. Sci. Technol.* 42, 4982–4988.
- Mahmood, J., Park, J., Shin, D., Choi, H.-J., Seo, J.-M., Yoo, J.-W., and Baek, J.-B. (2018). Organic ferromagnetism: trapping spins in the glassy state of an organic network structure. *Chem* 4, 2357–2369.
- Makino, K., Mossoba, M.M., and Riesz, P. (1982). Chemical effects of ultrasound on aqueous-solutions - evidence for .OH and .H by spin trapping. *J. Am. Chem. Soc.* 104, 3537–3539.
- Mas-Torrent, M., Crivillers, N., Rovira, C., and Veciana, J. (2012). Attaching persistent organic free radicals to surfaces: how and why. *Chem. Rev.* 112, 2506–2527.
- Nefedov, V.I., Firsov, M.N., and Shaplygin, I.S. (1982). Electronic-structures of  $\text{MRhO}_2$ ,  $\text{MRh}_2\text{O}_4$ ,  $\text{RhMO}_4$  and  $\text{Rh}_2\text{MO}_8$  on the basis of X-ray spectroscopy and ESCA data. *J. Electron. Spectrosc. Relat. Phenom.* 26, 65–78.
- Nishinaga, A., Shimizu, T., and Matsuura, T. (1977). Reaction of potassium superoxide with phenoxy radicals - mechanism of base-catalyzed oxygenation of phenols. *Chem. Lett.* 547–550.
- Pryor, W.A., Prier, D.G., and Church, D.F. (1983). Electron-spin resonance study of mainstream and sidestream cigarette-smoke - nature of the free-radicals in gas-phase smoke and in cigarette tar. *Environ. Health Perspect.* 47, 345–355.
- Rosen, G.M., and Rauckman, E.J. (1981). Spin trapping of free-radicals during hepatic-microsomal lipid-peroxidation. *Proc. Natl. Acad. Sci. U S A* 78, 7346–7349.
- Schummer, C., Groff, C., Al Chami, J., Jaber, F., and Millet, M. (2009). Analysis of phenols and nitrophenols in rainwater collected simultaneously on an urban and rural site in east of France. *Sci. Total Environ.* 407, 5637–5643.
- Sedo, J., Saiz-Poseu, J., Busque, F., and Ruiz-Molina, D. (2013). Catechol-based biomimetic functional materials. *Adv. Mater.* 25, 653–701.
- Shin, G., 이상일, Choi, S., Kim, J., and Weon, k. (2020). Degradation characteristics and upgrading biodegradability of phenol by dielectric barrier discharge plasma using catalyst materials. *J. Korean Soc. Water Wastewater* 34, 75–83.
- Steelink, C. (1965). Stable phenoxy radicals derived from phenols related to lignin. *J. Am. Chem. Soc.* 87, 2056.
- Sugama, T., Kukacka, L.E., Carciello, N., and Hocker, N.J. (1989). Study of interactions at water-soluble polymer  $\text{Ca}(\text{OH})_2$  or gibbsite interfaces by XPS. *Cem. Concr. Res.* 19, 857–867.
- Sun Yugang, C.H., Li, Yinghui, and Lin, Xiangqin (2000). Determination of some catechol derivatives by a flow injection electrochemiluminescent inhibition method. *Talanta* 53, 661–666.
- Tong, H., Lakey, P.S.J., Arangio, A.M., Socorro, J., Kampf, C.J., Berkemeier, T., Brune, W.H., Poschl, U., and Shiraiwa, M. (2017). Reactive oxygen species formed in aqueous mixtures of secondary organic aerosols and mineral dust influencing cloud chemistry and public health in the Anthropocene. *Faraday Discuss* 200, 251–270.
- Trinh, Q.T., Bhola, K., Amaniampong, P.N., Jérôme, F., and Mushrif, S.H. (2018). Synergistic application of XPS and DFT to investigate metal oxide surface catalysis. *J. Phys. Chem. C* 122, 22397–22406.
- Valavanidis, A., Fiotakis, K., Bakeas, E., and Vlahogianni, T. (2013). Electron paramagnetic resonance study of the generation of reactive oxygen species catalysed by transition metals and quinoid redox cycling by inhalable ambient particulate matter. *Redox Rep.* 10, 37–51.
- Vandoveren, H., and Verhoeven, J.A.T. (1980). XPS spectra of Ca, Sr, Ba and their oxides. *J. Electron. Spectrosc. Relat. Phenom.* 21, 265–273.
- Vejerano, E., Lomnicki, S., and Dellinger, B. (2011). Formation and stabilization of combustion-generated environmentally persistent free radicals on an  $\text{Fe}(\text{III})_2\text{O}_3$ /silica surface. *Environ. Sci. Technol.* 45, 589–594.
- Veres, P., Roberts, J.M., Burling, I.R., Warneke, C., de Gouw, J., and Yokelson, R.J. (2010). Measurements of gas-phase inorganic and organic acids from biomass fires by negative-ion proton-transfer chemical-ionization mass spectrometry. *J. Geophys. Res.* 115, 15.
- Wang, Q., Zhang, X., Sun, S.P., Wang, Z.C., and Cui, D. (2020). Effect of Cao on pyrolysis products and reaction mechanisms of a corn stover. *ACS Omega* 5, 10276–10287.
- Wiechen, M., Zaharieva, I., Dau, H., and Kurz, P. (2012). Layered manganese oxides for water-oxidation: alkaline earth cations influence catalytic activity in a photosystem II-like fashion. *Chem. Sci.* 3, 2330–2339.
- Xie, Z., Tian, D., Xie, M., Yang, S.-Z., Xu, Y., Rui, N., Lee, J.H., Senanayake, S.D., Li, K., Wang, H., et al. (2020). Interfacial active sites for  $\text{CO}_2$  assisted selective cleavage of C-C/H bonds in ethane. *Chem* 6, 2703–2716.
- Xu, W.M., Rong, M.Z., and Zhang, M.Q. (2016). Sunlight driven self-healing, reshaping and recycling of a robust, transparent and yellowing-resistant polymer. *J. Mater. Chem. A* 4, 10683–10690.
- Yang, L., Liu, G., Zheng, M., Jin, R., Zhu, Q., Zhao, Y., Wu, X., and Xu, Y. (2017a). Highly elevated levels and particle-size distributions of environmentally persistent free radicals in haze-associated atmosphere. *Environ. Sci. Technol.* 51, 7936–7944.
- Yang, L., Liu, G., Zheng, M., Zhao, Y., Jin, R., Wu, X., and Xu, Y. (2017b). Molecular mechanism of dioxin formation from chlorophenol based on electron paramagnetic resonance spectroscopy. *Environ. Sci. Technol.* 51, 4999–5007.

iScience, Volume 24

## **Supplemental information**

### **Photoinduced formation of persistent free radicals, hydrogen radicals, and hydroxyl radicals from catechol on atmospheric particulate matter**

**Linjun Qin, Lili Yang, Jiahui Yang, Ralph Weber, Kalina Rangelova, Xiaoyun Liu, Bingcheng Lin, Cui Li, Minghui Zheng, and Guorui Liu**

## Supplemental Information

### Transparent Methods

#### Materials

Catechol (purity > 99%) was purchased from J&K Scientific Ltd. (Beijing, China) and used as received without further treatment or purification. Phosphate-buffered saline (0.01 M, pH 7.4, 0.138 M NaCl and 0.0027 M KCl) was purchased from Solarbio Science & Technology Co., Ltd (Beijing, China). 5,5-Dimethyl-1-pyrroline-*N*-oxide (DMPO, purity > 99.99%, GC grade) was obtained from Dojindo Laboratories and used without additional purification. Three metal oxides commonly found in the natural environment were purchased. These were  $\alpha$ -Fe<sub>2</sub>O<sub>3</sub> (purity 99.55%; Macklin Biochemical Technology Co., Ltd, Shanghai, China), CuO (Alfa Aesar China, Shanghai, China), and CaO (purity 98%; Sigma–Aldrich, St. Louis, MO). Silica (100–200 mesh size, J&K Scientific Ltd) was used as an inert substrate for mixing with the metal oxide and chemical precursor. Experiments were prepared by loading catechol (5% mass fraction) and metal oxide (5% mass fraction) /SiO<sub>2</sub> into the EPR quartz tube (internal diameter = 4 mm, external diameter = 5 mm, length = 10 cm) to a height of 1 cm. The quartz tube was putted into the cavity of the EPR spectrometer for detection the formation of free radicals during photochemical reactions.

The formation reactions of free radicals were trigged by in situ light irradiation. A 100 W mercury arc lamp (LOT-Oriel GmbH & Co. KG, Germany) was used as the light source (wavelength: 200–2000 nm) to simulate UV irradiation. Visible light experiments

were conducted with in situ irradiation and direct offline irradiation with a 500 W short arc spherical xenon lamp (CHF-XM 500, Beijing Perfect Light Technology Co., Ltd Beijing, China) with a wavelength range of 400–700 nm.

### **Sampling of ambient PM<sub>2.5</sub> as a matrix for photochemical formation**

To simulate the formation of free radicals from catechol under light irradiation in the atmosphere and evaluate the effect of PM<sub>2.5</sub> on free radical formation, real PM<sub>2.5</sub> samples were collected and used as the matrix for photochemical formation of free radicals. Low-volume air samplers (LVS3, Sven Leckel Ingenieurbüro GmbH, Berlin, Germany) with a flow rate of 2.3 m<sup>3</sup>/h were used to collect ambient PM<sub>2.5</sub> samples. The sampling site was located in an ecological monitoring station in Beijing (40°26.88'N, 116°20'13.89'E), and situated approximately 110 m away from a road. Samples were collected on quartz fiber filters (ø47 mm, Whatman, Maidstone, UK), which were baked at 450 °C for 12 h to remove organic contaminants before use. Sampling of PM<sub>2.5</sub> was conducted continuously for approximately 72 h to capture sufficient airborne PM<sub>2.5</sub>. After collection of PM<sub>2.5</sub>, the quartz fiber filters were wrapped in aluminum foil and stored at -18 °C.

For analysis, the quartz filters with collected PM<sub>2.5</sub> were cut into small pieces using ceramic scissors and then mixed. Samples were prepared by adding 4 mg (10% mass fraction) of catechol to 40 mg of PM<sub>2.5</sub> filters, followed by vortex mixing to homogenize and then placed 20mg sample into the EPR quartz tube (internal diameter = 4 mm, external diameter = 5 mm, length = 10 cm) to a height of 0.5 cm.

## **Electron paramagnetic resonance spectroscopy parameters**

Electron paramagnetic resonance spectroscopy (EPR) is the most direct detection technique for free radicals and was used in this study to monitor the formation of free radicals from catechol. EPR was conducted using a Bruker EMX-plus X-band EPR spectrometer (Bruker Instruments, Billerica, MA). The parameters for detecting EPRs in solid phase samples were set as follows: microwave frequency, 9.78 GHz; modulation frequency, 100 kHz; modulation amplitude, 1.0 G; receiver gain, 30 dB; center field, 3500 G; sweep width, 100 G; time constant, 40.96 ms; sweep time, 100 s; and microwave power, 0.63 mW.

The EPR operating parameters for detecting hydroxyl radicals ( $\bullet\text{OH}$ ), hydrogen ( $\bullet\text{H}$ ), and superoxide anions ( $\text{O}_2^{\bullet-}$ ) were set as follows: microwave frequency, 9.78 GHz; modulation frequency, 100 kHz; modulation amplitude, 1.0 G; receiver gain, 30 dB; center field, 3500 G; sweep width, 200 G; time constant, 2.62 ms; sweep time, 10 s; and microwave power, 20 mW.

## **Sample characterization**

X-ray photoelectron spectroscopy (XPS) was used to characterize changes in the metal oxides before and after the photochemical reactions. XPS (ESCALAB 250Xi, Thermo Fisher Scientific) was used to characterize the valence states and compositions of metal compounds using a monochromatic light source (Al-K $\alpha$  source,  $h\nu = 1486.6$  eV) with a pass energy of 40 eV. A step size of 0.05 eV was used and the binding energy was corrected using the C 1s peak (284.6 eV) as a reference. The morphologies and elemental

compositions of PM<sub>2.5</sub> before and after UV irradiation were investigated with scanning electron microscopy with energy dispersive X-ray spectroscopy (SEM-EDX, HITACHI S-3000N).

## Supplemental Data Items

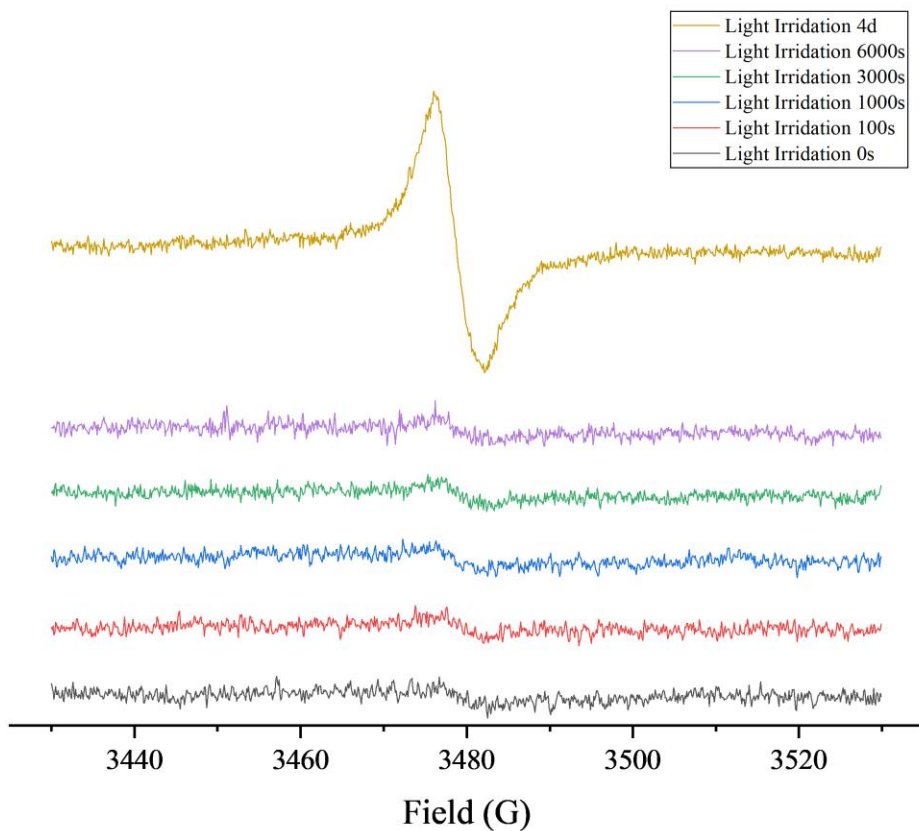


**Figure S1.** Changes in electron spin resonance spectra over time under continuous visible light irradiation for 5% Fe(III)<sub>2</sub>O<sub>3</sub>/silica loaded with catechol (5%). Related to Figure 1.

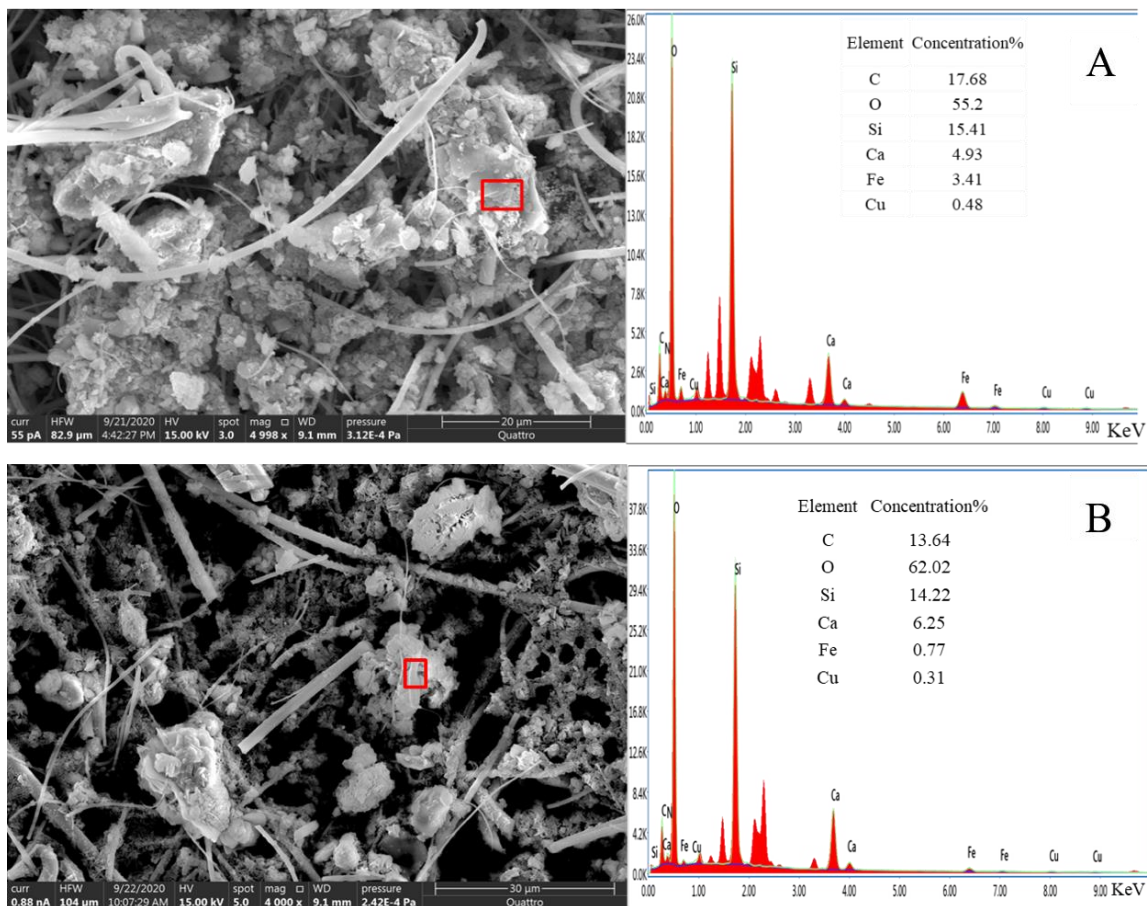


**Figure S2.** Energy dispersive X-ray spectra of (A) PM<sub>2.5</sub> and (B) PM<sub>2.5</sub>-UV and their elemental compositions. Related to Figure 2.

Large, spherical, irregular, and porous atmospheric particulate matter was observed by SEM. It is likely that pollutants like phenols could absorb on the surfaces of particles with large surface areas. EDX was used to detect C, O, N, Si, Ca, Fe, and Cu in the PM<sub>2.5</sub>. The results indicated the presence of some organic compounds, inorganic inert fragments, and metals in the atmospheric particulate matter. After UV irradiation, the oxygen content in the particulate matter increased, which indicated that some organic compounds were oxidized under UV irradiation.

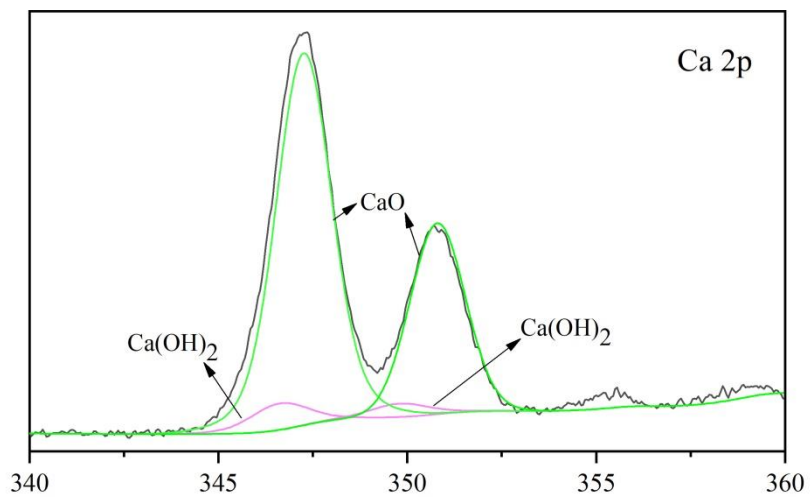


**Figure S3.** Deconvolution of the Ca 2p spectra of catechol/CaO/SiO<sub>2</sub> before UV irradiation. Related to Figure 3.

**Table S1.** Average *g*-values of the deconvoluted EPR spectra of the samples. Related to Figure 7.

Samples	Energy Type	<i>g</i> <sub>1</sub>	<i>g</i> <sub>2</sub>	<i>g</i> <sub>3</sub>
		UV Irradiation for 5500s		
<b>CT-SiO<sub>2</sub></b>	UV	/	2.00453	2.00571
Mainly species of free radicals			Oxygen-center semiquinone radical	Oxygen-center semiquinone radical
Peak area ratio			99.97%	0.03%
<b>CT-Fe<sub>2</sub>O<sub>3</sub>-SiO<sub>2</sub></b>	UV	2.00131	2.00359	2.00501
Mainly species of free radicals		F-Center	Oxygen-center phenoxy radical	Oxygen-center semiquinone radical
Peak area ratio		1.36%	12.36%	86.28%
<b>CT-CuO-SiO<sub>2</sub></b>	UV	2.00148	2.00405	2.00518
Mainly species of free radicals		F-Center	Oxygen-center phenoxy radical	Oxygen-center semiquinone radical
Peak area ratio		2.72%	12.90%	84.38%
<b>CT-CaO-SiO<sub>2</sub></b>	UV	2.00119	2.00487	2.00759
Mainly species of free radicals		F-Center	Oxygen-center semiquinone radical	Oxygen-center semiquinone radical
Peak area ratio		0.03%	99.52%	0.45%

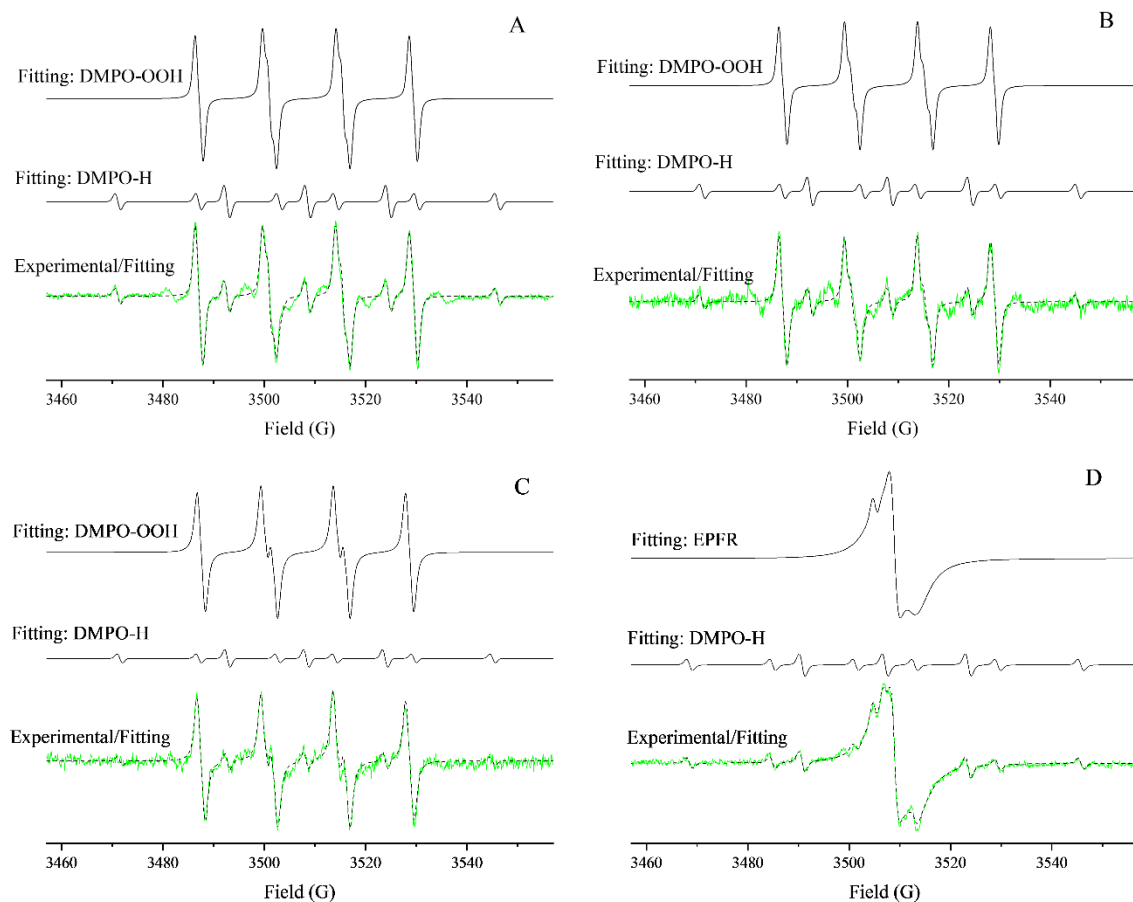


**Figure S4.** Fitting of the EPR spectra of spin-trapped radicals detected in the solid-phase of (A) catechol (CT)/SiO<sub>2</sub> under UV irradiation, (B) CT/Fe<sub>2</sub>O<sub>3</sub>/SiO<sub>2</sub> under UV irradiation, (C) CT/CuO/SiO<sub>2</sub> under UV irradiation, (D) CT/CaO/SiO<sub>2</sub> under UV irradiation. Related to Figure 5E.

After deconvolution of EPR spectrum, a second very small hyperfine splitting  $\alpha_{\text{H}}^{\beta 1}$  = 0.8 G was shown in our system (Figure S4) which emphasized the production of superoxide radicals. And this second hyperfine splitting sometimes was not well resolved if the spectra were slightly overmodulated.

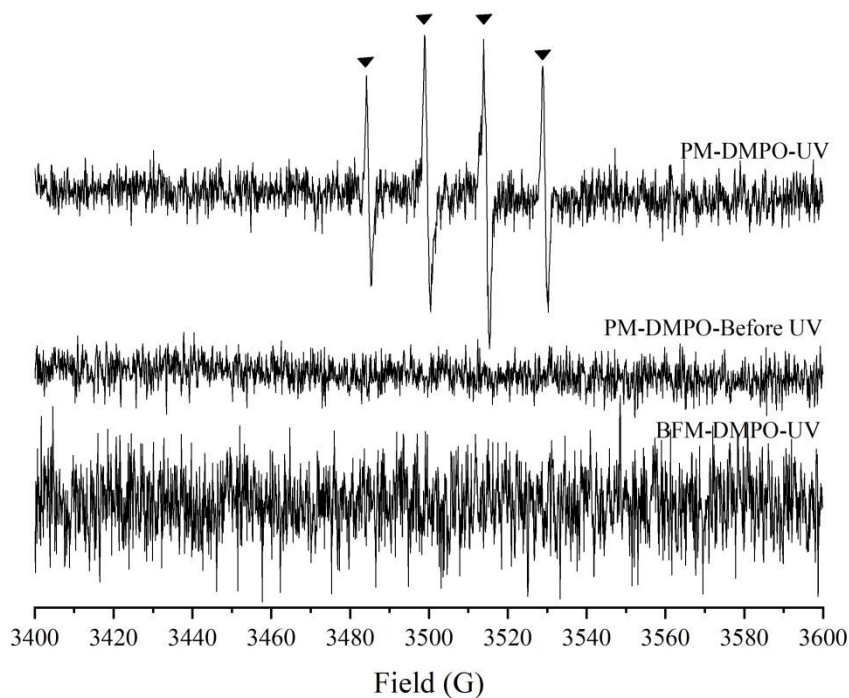


**Figure S5.** 2  $\mu\text{L}$ , 3 M DMPO/water + 30  $\mu\text{L}$ , PBS + 1 mg  $\text{PM}_{2.5}$ /UV irradiation. Control experiments: 2  $\mu\text{L}$ , 3 M DMPO/water + 30  $\mu\text{L}$ , PBS + 1 mg BFM/UV irradiation. This was a repeatability test and the  $\text{PM}_{2.5}$  used differed to that used to obtain the results shown in Figure. 5D. Related to Figure 5D.

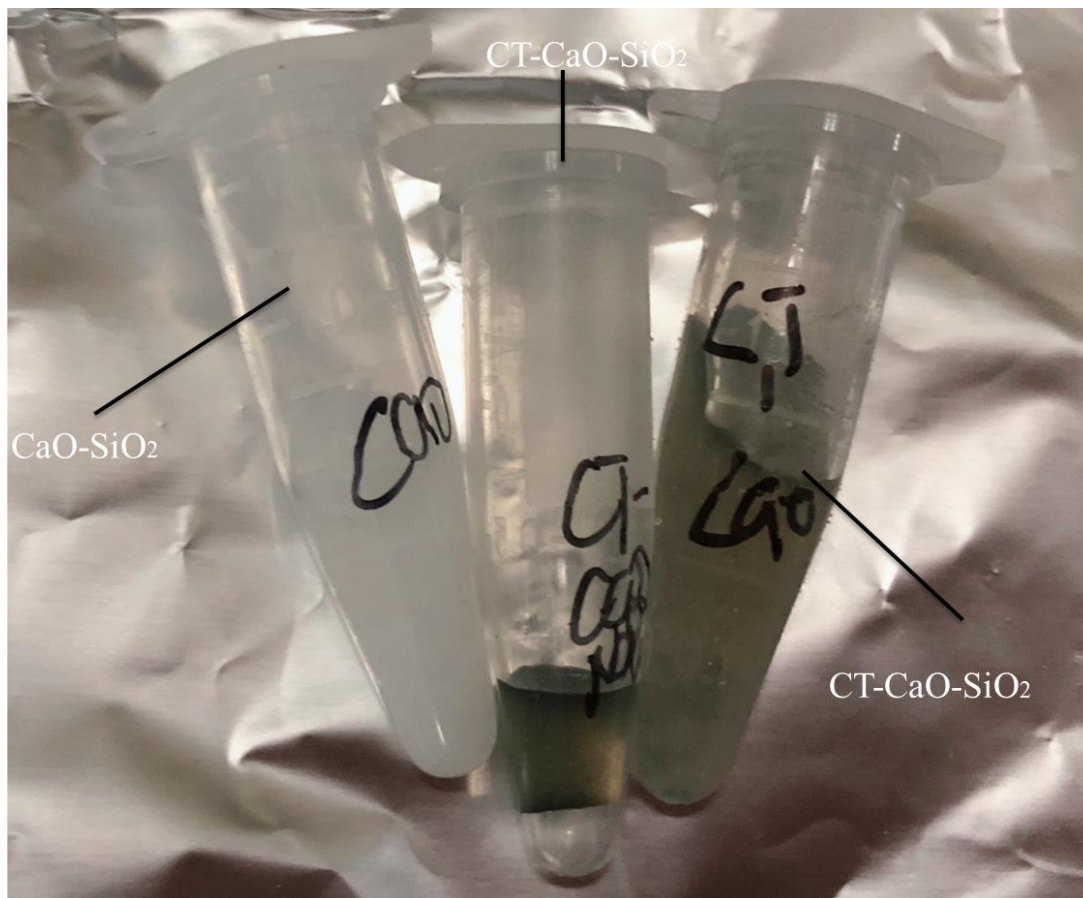


**Figure S6.** Formation of the F-center in catechol–CaO–SiO<sub>2</sub> and associated color changes, which were similar to those for alkali halides. Related to Figure 7.

The F-center formed in CaO was similar to that for alkali halides and different from those for heavy metal oxides (CuO and Fe<sub>2</sub>O<sub>3</sub>).

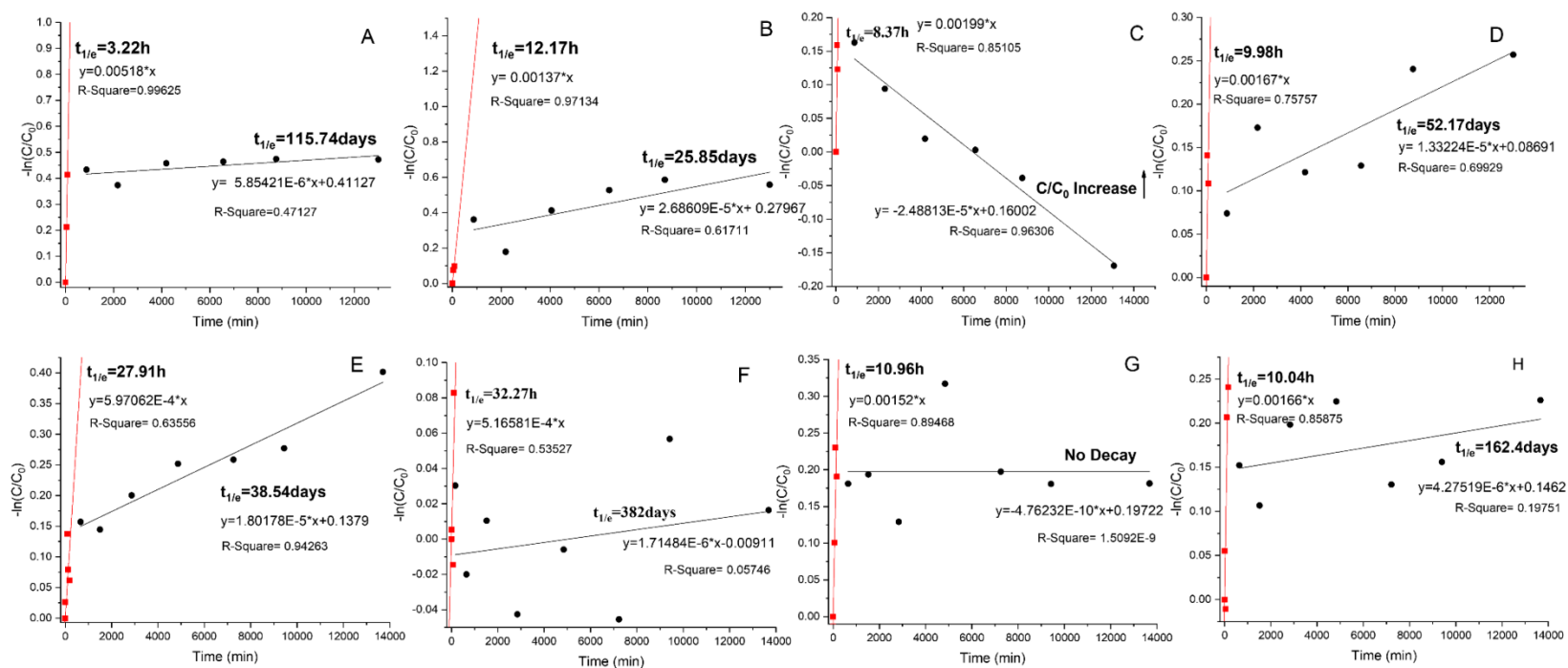


**Figure S7.** The half-lives of experimental samples after light irradiation for 5500 s. (A) catechol (CT)/PM, (B) CT/BFM, (C) CT/CaO/PM, (D) PM, (E) CT/CuO/SiO<sub>2</sub>, (F) CT/CaO/SiO<sub>2</sub>, (G) CT/Fe<sub>2</sub>O<sub>3</sub>/SiO<sub>2</sub>, and (H) CT/SiO<sub>2</sub>. Related to Figure 1 and Figure 2.